analytical chemistry

Article

pubs.acs.org/ac

Heterogeneous Nano Metal–Organic Framework Fluorescence Probe for Highly Selective and Sensitive Detection of Hydrogen Sulfide in Living Cells

Yu Ma, Hao Su, Xuan Kuang, Xiangyuan Li, Tingting Zhang, and Bo Tang*

College of Chemistry, Chemical Engineering and Materials Science, Collaborative Innovation Center of Functionalized Probes for Chemical Imaging, Key Laboratory of Molecular and Nano Probes, Ministry of Education, Shangdong Provincial Key Laboratory of Clean Production of Fine Chemicals, Shandong Normal University, Jinan 250014, People's Republic of China

Supporting Information

ABSTRACT: Hydrogen sulfide (H_2S) has been regarded as the third important gaseous signaling molecule involved in human physiological and pathological processes. Due to the high reactive and diffusible properties of H_2S, real-time detection of H_2S fluctuations in living biological specimens is crucial. Here, we present a Cu(II)-metalated 3D porous nanoscale metal–organic framework (nano-MOF) $\{CuL\text{-}[AlOH]_2\}_n$ (PAC; H_6L = *meso*-tetrakis(4-carboxylphenyl)porphyrin) and successfully employ this nano-MOF as a novel heterogeneous fluorescence probe for H_2S detection. As far as we know, nano-MOFs have never been used as selective fluorescence probes for H_2S detection. On the basis of the advantages of nano-MOF materials, this biocompatible nano-MOF probe exhibits rapid response, excellent selectivity, and hypotoxicity in in situ detection of H_2S and represents the most sensitive fluorescence probe for selective H_2S detection under physiological pH. In addition, confocal imaging was achieved successfully in living cells.

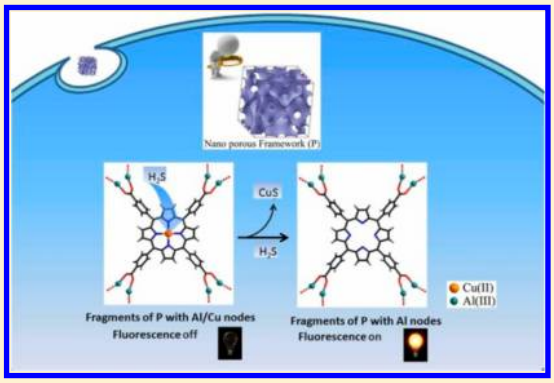

Hydrogen sulfide (H_2S) has attracted great attention for its recently established function as a signal transmitter in living organisms.[1,2] It has been regarded as the third important gaseous signaling molecule following nitric oxide (NO) and carbon monoxide (CO).[1−4] The endogenous H_2S, mainly biosynthesized by enzymatic reactions,[5] has been found to be involved in many physiological processes, such as antioxidation,[6] anti-inflammation,[7] and apoptosis.[8] In addition, abnormal concentrations of H_2S have also been correlated with many pathological processes, such as Alzheimer's disease[9] and Down's syndrome.[10] To better understand the contributions of H_2S in these processes, it is crucial to monitor the H_2S level with spatial and temporal information in living cells and organisms. However, due to the high reactive and diffusible properties of H_2S, the traditional detection technologies, such as gas chromatography,[11,12] and colorimetric[13,14] and electrochemical[15,16] analysis, are not appropriate for real-time detection. They often require a complicated postmortem process and/or even destruction of tissues or living cells. Fortunately, the fluorescence-probe-based fluorescence imaging technology was born at the right time. Owing to the advantages of high selectivity and sensitivity and good compatibility for various biosamples of this technology,[17−19] the design and synthesis of fluorescence probes for H_2S detection has inspired great interest in this field.

Recently, a certain amount of turn-on type fluorescence probes for detection of H_2S have been reported, and the design strategies mainly rely on the typical reactive characteristics of H_2S, including H_2S-mediated hydroxyl amide, nitro, and azide reduction,[20−30] dual nucleophilic addition,[31−36] copper sulfide precipitation,[37−40] and thiolysis of dinitrophenyl ether.[41,42] These unique reactive properties can efficiently distinguish H_2S from other biological species; however, the study of novel H_2S probes is still needed because of the complexity of studying the underlying molecular events involved in signaling transduction, and other problems related to the probes, such as their resistance to thiol interference, response times (typically 20 min to 2 h), detection limit, quantity control of the probe in cells, the presence of toxic organic cosolvents, etc.

In the past few decades, metal–organic frameworks (MOFs), as a new type of porous coordination compounds, have been studied extensively. On the basis of the properties of controllable synthesis, structural diversity, porosity, high specific surface areas, metal active site richness, and flexibility of the pore size/wall modification, these materials have shown great potential applications in gas storage, catalysis, chemical sensing, optics, and biological applications, etc.[43−46] Attractively, the past studies also revealed that the size of the MOFs can also be decreased to the nanoscale, and these nanoscale MOFs often provide a significant performance improvement over their bulk crystals in these applications.[47] For example, a recently reported nanoscale MOF

Received: September 26, 2014
Accepted: October 24, 2014
Published: October 24, 2014

   dx.doi.org/10.1021/ac503622n | *Anal. Chem.* 2014, 86, 11459–11463

probe could recognize H_2S and cysteine over other amino acids.[48] However, the nano-MOFs have never been used as selective fluorescence probes for H_2S detection.

Herein we intend to develop of a novel heterogeneous nano-MOF probe for H_2S detection. The key point of the probe design is how to introduce the reactive site for H_2S into the framework. Considering the flexibility of functionalization for MOFs, the design can be achieved by introduction of active metal centers, ligand functionalization, or postmodification, which presages the huge potential for MOFs in probe design. Here, we only selected a simple strategy by introducing reactive metal centers (Cu(II) ions) into the framework as the H_2S-responding site and synthesized a 3D porous nanoscale aluminum−copper mixed-metal MOF $\{CuL[AlOH]_2\}_n$ (referred to as PAC; H_6L = *meso*-tetrakis(4-carboxylphenyl) porphyrin) as a novel H_2S fluorescence probe (Figure 1). Combining the unique properties of

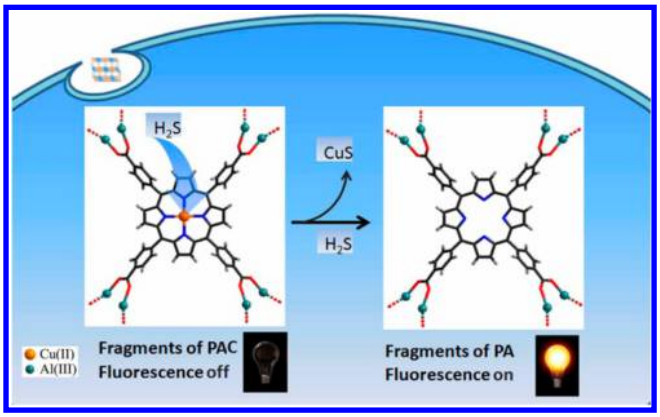

Figure 1. Structural fragment of nano-MOF PAC and the proposed strategy for fluorescent variation of PAC upon reactive metal centers (Cu(II) ions) as the H_2S-responding site. The corresponding product is referred to as luminophor nano-MOF PA.

MOFs (such as porosity, high specific surface areas, abundant host−guest interactions, the inherent confinement effect within the pores, and metal active site richness) and advantages of nanoscale materials (such as ease of implementing probe endocytosis and abilitiy to avoid exosmosis of small organic molecule probes together with an increasing reservation amount of the probe), this biocompatible nano-MOF probe exhibits rapid response, excellent selectivity, and hypotoxicity in in situ detection of H_2S and represents the most sensitive fluorescence probe for selective H_2S detection under physiological pH. In addition, confocal imaging was achieved successfully in living cells.

EXPERIMENTAL SECTION

Materials. The reagents were obtained from commercial sources and used without further purification. Pyrrole, 4-formylbenzoic acid, copper acetate, aluminum trichloride, sodium hydrosulfide, glutathione (GSH), cysteine (Cys), homocysteine (Hcy), hydrogen peroxide (H_2O_2; 30% aqueous solution), Dulbecco's modified Eagle's medium (DMEM), 3-(4,5-dimethylthiazol-2-yl)-2,5-diphenyltetrazolium bromide (MTT), *S*-nitroso-*N*-acetyl-DL-penicillamine (SNP; the source of NO), and other relevant inorganic compounds (KSCN, Na_2SO_4, Na_2SO_3, $Na_2S_2O_3$, NaClO, Na_2HPO_4, NaH_2PO_4, and $NaHCO_3$) were purchased from Sigma-Aldrich (Shanghai, China). Hoechst 33342 was obtained from the Beyotime Institute of Biotechnology (Shanghai, China). Ultrapure water (18.2 MΩ cm) was obtained from a Water Pro water purification system (Labconco Corp., Kansas City, MO). HepG2 cells (human hepatocellular liver carcinoma cells) and A549 cells (human lung carcinoma cells) were purchased from the Committee on Type Culture Collection of the Chinese Academy of Sciences.

Physical Measurements. Powder X-ray diffraction (PXRD) patterns were measured at room temperature (298 K) on a Bruker SMART APEX charge-coupled device (CCD)-based diffractometer. ^1H NMR spectra were taken on a nuclear magnetic resonance spectrometer (AVANCE 300, Bruker, Switzerland). The FT-IR (KBr pellet) spectrum was recorded (400−4000 cm^{-1} region) on a Nicolet Magna 750 FT-IR spectrometer. Transmission electron microscopy (TEM) images were taken on a JEM-1011 electron microscope (JEOL, Japan) at an accelerating voltage of 100 kV. Energy dispersive spectroscopy (EDS) mapping analysis was carried out on a SUPRA 55 scanning electron microscope. The fluorescence spectra were determined on a spectrofluorometer (FLS-920, Edingburgh). Absorbance was measured on a microplate reader (RT-6000, Rayto, Guangdong, China) in the MTT assay. The fluorescence kinetics was recorded on a Cary Eclipse spectrofluorometer (Varian, Australia) with a xenon lamp. All pH measurements were carried out by a pH-3c digital pH meter (Shanghai Lei Ci Device Works, Shanghai, China) with a combined glass−calomel electrode. The fluorescence images of the cells were recorded by a confocal laser scanning microscope (TCS SP5, Leica, Wetzlar, Germany) with an excitation wavelength of 405 nm.

Synthesis of Ligand L and Nano-MOF PAC. The organic ligand *meso*-tetrakis(4-carboxylphenyl)porphyrin (H_6L) was synthesized according to the literature.[21] First, 4-formylbenzoic acid (3.0 g, 0.02 mol) was added to a solution of propionic acid (200 mL) in pyrrole (1.39 mL, 0.02 mol). Next, the mixture was heated to reflux for 1 h. After cooling, a brown-purple precipitate formed. The precipitate was isolated by filtration, washed with CH_2Cl_2, and then dried under vacuum for 6 h. ^1H NMR (DMSO-d_6, 300 MHz): 8.08 (m, 8H), 8.27 (m, 8H), 8.87 (br, 8H).

A mixture of $AlCl_3{\cdot}6H_2O$ (0.0125 mmol, 0.030 g), H_6L (0.063 mmol, 0.050 g), and cetyltrimethylammonium bromide (CTAB) (1 mmol, 0.036 g) in water (5 mL) was stirred for 10 min at room temperature and then heated in a 23 mL Teflon-lined autoclave at 180 °C for 16 h. After being cooled to room temperature slowly, the purple nanoscale crystals (referred to as nano-precursor PA) were collected by centrifugal separation and washed with DMF, H_2O, and acetone in turn for several times, yield 39%. Then a mixture of the activated PA (170 °C under vacuum, overnight) (50 mg) and $Cu(Ac)_2{\cdot}6H_2O$ (0.2 mmol, 0.050 g) in DMF (5 mL) was stirred for 10 min at room temperature and then heated in a 23 mL Teflon-lined autoclave at 100 °C for 24 h. After being cooled to room temperature slowly, the sample was also collected by centrifugal separation and washed with DMF, H_2O, and acetone in turn several times, yield 90%. The phase purity of the samples and the Cu(II) insertion rate at the center of the porphyrin were confirmed by PXRD, FT-IR, and EDS.

Cell Culture. HepG2 cells and A549 cells were maintained following the protocols provided by the American Type Tissue Culture Collection. HepG2 cells were incubated in high-glucose DMEM (4.5 g of glucose/L) supplemented with 10% fetal bovine serum (FBS), $NaHCO_3$ (2 g/L), and 1% antibiotics (penicillin/streptomycin, 100 U/mL). A procedure similar to that for HepG2 cells was followed to culture the A549 cells,

dx.doi.org/10.1021/ac503622n | *Anal. Chem.* 2014, 86, 11459−11463

except the DMEM was replaced by 1640 medium. The cultures were maintained in a humidified incubator in 5% CO_2/95% air at 37 °C. HepG2 and A549 cells were both passed and plated on 18 mm glass coverslips in a culture dish and maintained for 1 day at 37 °C and 5% CO_2 before imaging.

Confocal Imaging. After HepG2 cells were cultured on coverslips in a culture dish for 24 h, the probe PAC (10 μM) was delivered into the cells in DMEM medium containing 10% FBS at 37 °C for 1 h. The cells were then washed three times with 20 mM boric acid−borax buffer (referred to as BBS). Then confocal laser scanning microscopy (CLSM) with 405 nm excitation was performed with a He−Ne laser, and the emission was collected between 580 and 680 nm. A procedure similar to that for HepG2 cells was followed for the confocal imaging of A549 cells, except the DMEM was replaced by 1640 medium.

In the case of costaining HepG2 cells with PAC and a nucleus -specific dye (Hoechst 33342), HepG2 cells were first coincubated with DMEM containing 10% FBS, 10 μM PAC, and 500 μM Hoechst 33342 at 37 °C for 1 h and then washed with BBS three times. Then CLSM with 405 nm excitation was performed, and the emission was recorded between 580 and 680 nm and between 410 and 480 nm, respectively.

MTT Assay. HepG2 cells (10^5 cells·mL^{-1}) were dispersed within replicate 96-well microtiter plates to a total volume of 200 μL·well^{-1}. The plates were maintained at 37 °C in a 5% CO_2/95% air incubator for 12 h. The cells were sequentially incubated with different concentrations of PAC (10, 30, 50, 100, and 200 μM) for another 24 h. An MTT solution (5.0 mg·mL^{-1}, BBS) was then added to each well. After 4 h, the remaining MTT solution was removed, and 150 μL of DMSO was added into each well to dissolve the formazan crystals. The absorbance was measured at 490 nm in a TRITURUS microplate reader.

RESULTS AND DISCUSSION

Preparation and Characterization of the Nano-MOF. The nanoscale aluminum−copper mixed-metal MOF PAC ($\{CuL[AlOH]_2\}_n$) was obtained from Cu(II) metalation of the porphyrin ring within the rigid host structure of the fluorescence nano metal−organic framework $\{H_2L[AlOH]_2\text{-}(DMF)_3(H_2O)_2\}_n$ (referred to as PA). The synthesis mainly benefits from the consideration that Cu(II) ions are preferably coordinated with nitrogen atoms in the nitrogen-bearing macrocyclic ligands.[49] PAC maintained a stable noninterpenetrated 3D porous framework as PA, but the paramagnetic characteristics of the Cu(II) ions quenched the ligand-based fluorescence completely as expected. When H_2S appeared, the Cu(II) ions were taken from the porphyrin centers, and the luminophor nano-MOF PA was, thus, obtained simultaneously.

Nano-MOF PA was prepared according to the literature for bulk crystals of PA and other nanomaterials by adding the surfactant CTAB,[50,51] and the purity of the as-synthesized sample was demonstrated by PXRD (Figure S1, Supporting Information). PAC was metalated by the reaction of $Cu(Ac)_2\cdot H_2O$ with activated nano-PA in water under hydrothermal conditions at 100 °C. The PXRD pattern for PAC obtained in the same conditions is coincident with that for the as-synthesized sample of PA, suggesting that Cu metalation does not destroy the stable framework of PA (Figure S1). The EDS spectrum gives an Al/Cu ratio of 2, consistent with 100% occupancy of the porphyrin center by Cu(II) ions (Figure S2, Supporting Information). All these results reveal that PAC also crystallizes in the space group *Cmmm* and exhibits noninterpenetrated three-dimensional porous frameworks. The Al(III) center is six-coordinated by four equatorial carboxylate oxygen atoms from four different L ligands and two axial μ_2-OH^- bridges. Adjacent metal ions are doubly bridged by these two μ_2-OH^- bridges to generate a 1D $Al(OH)O_4$ chain. Each porphyrin linker with the center site occupied by Cu(II) ions is coordinated to eight Al(III) centers through the four carboxylate groups and interconnects 1D $Al(OH)O_4$ chains to give a complicated 3D porous framework.

Spectroscopic Properties of PAC toward H_2S. Subsequently, we investigated the spectroscopic properties of PAC. This nanoprobe with an average size of 60 nm being characterized by TEM (Figure S3, Supporting Information) shows fine aqueous dispersibility and no need for toxic organic cosolvent. As can be seen from Figure 2, upon treatment of 10 μM PAC with 100 μM NaHS in aqueous solutions buffered at physiological pH (BBS, pH 7.4), a significant fluorescence enhancement was observed. To further evaluate the efficiency of the probe in the measurement of the H_2S level, varying concentrations of NaHS (0−100 μM) were added to the solutions of PAC (10 μM). An excellent linear correlation between the fluorescence intensities and the added NaHS concentrations was observed (Figure S4, Supporting Information). The detection limit for H_2S was found to be about 16 nM, comparable to that of the most sensitive H_2S-sensing fluorescence probe HS−Cy that has been reported by our group.[36] Beyond that, this new nano-MOF probe avoided the needs for improving the reaction rate by enhancing the pH (8.0) and the complexity of two excitation processes in the fluorescence imaging based on the two-step reactive mechanism of HS−Cy. Therefore, this novel probe has become the most sensitive H_2S probe under physiological pH (7.4).

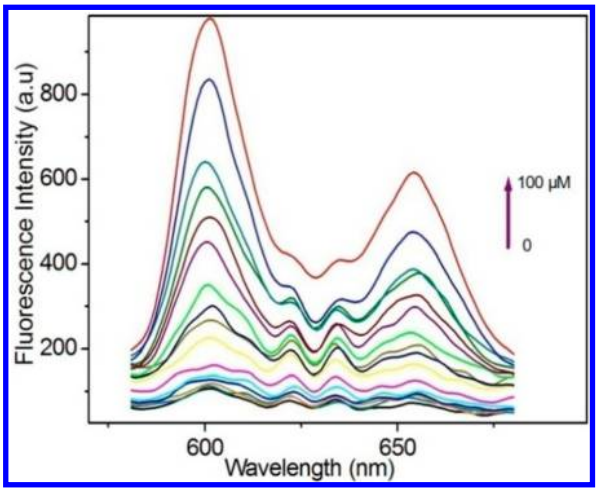

Figure 2. Fluorescence spectra of PAC (10 μM) in BBS butter (20 mM, pH 7.40) obtained upon titration with HS^- from 0 to 100 μM, λ_{ex} = 419 nm.

Selectivity and Reaction Kinetics of PAC toward H_2S. The experiments on selectivity were then carried out. As can be seen from Figure 3, compared with the large and immediate increment of fluorescence intensity upon addition of 100 μM NaHS, almost no fluorescence increment upon addition of abundant biologically relevant GSH (10 mM), whose levels are often higher than those of other thiols in the cells, was observed. We also examined other thiols and reactive individual oxygen/nitrogen species, such as Cys, Hcy, H_2O_2, ClO^-, and NO. Similarly, these species induced no obvious change in the fluorescence. Therein, such a large amount of interfering NO

dx.doi.org/10.1021/ac503622n | *Anal. Chem.* 2014, 86, 11459−11463

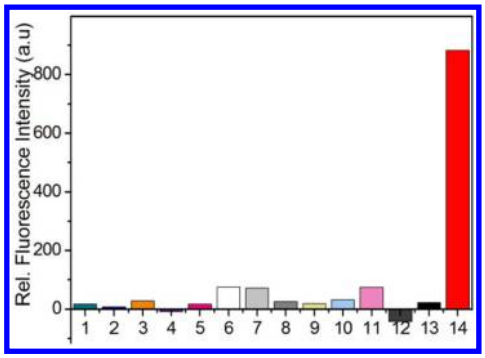

Figure 3. Fluorescence response of PAC toward various reactive species. Relative fluorescence intensity ($F - F_0$) on addition of (1) H_2O_2 (200 μM), (2) ClO^- (200 μM), (3) SCN^- (1 mM), (4) SO_4^{2-} (1 mM), (5) SO_3^{2-} (1 mM), (6) $S_2O_3^{2-}$ (1 mM), (7) Hcy (100 μM), (8) HPO_4^{2-} (1 mM), (9) $H_2PO_4^-$ (1 mM), (10) HCO_3^- (1 mM), (11) Cys (100 μM), (12) GSH (10 mM), (13) NO (10 mM), and (14) NaHS (100 μM), respectively. Data were obtained in BBS buffer (pH 7.4) with excitation at λ_{ex} = 419 nm.

(1000 equiv in concentration) has not yet been tested. Additionally, other interfering inorganic anions (SO_3^{2-}, $S_2O_3^{2-}$, SCN^-, SO_4^{2-}, HPO_4^{2-}, $H_2PO_4^-$, and HCO_3^-) were also examined, and they all showed no or very limited fluorescence responses. All these experimental results emphasized the probe's high selectivity toward H_2S in the living cells.

To further establish the possibility of real-time imaging of PAC for H_2S detection, we examined the response time of PAC to NaHS in BBS-buffered aqueous solution through the reaction kinetics. As can be seen from Figure S5 (Supporting Information), a significant fluorescence enhancement was observed instantaneously. All this proved that PAC is able to detect H_2S more rapidly and sensitively than most of the reported H_2S probes (typically 20 min to 2 h).

Luminescence Imaging of PAC in Living Cells. In view of the above results, we have reason to believe that the novel fluorescence probe PAC is promising for applications in biological imaging. We then evaluated the capability of the probe to detect exogenous H_2S in HepG2 cells. HepG2 cells were incubated with 10 μM PAC in DMEM for 30 min and then washed several times with Hanks' balanced salt solutions (HBSS). From Figure 4a, we cannot observe any significant fluorescence cells with only 10 μM PAC. The bright-field image is presented as Figure 4b. After 50 μM NaHS (the donor of H_2S) was coincubated, a large intracellular fluorescence enhancement was observed (Figure 4c), corresponding to the bright-field image (Figure 4d). Simultaneously, a costaining experiment of HepG2 cells with PAC and a nucleus-specific dye (Hoechst 33342) was conducted with a 405 nm excitation with emission bands of 410–480 and 580–680 nm, respectively. The good morphology of HepG2 cells after incubation with PAC for 1 h suggested satisfactory biocompatibility of the probe (Figure S6, Supporting Information). In addition, an MTT assay with HepG2 cells was performed (Figure S7, Supporting Information). All these results demonstrated that PAC was of low toxicity and high biocompatibility.

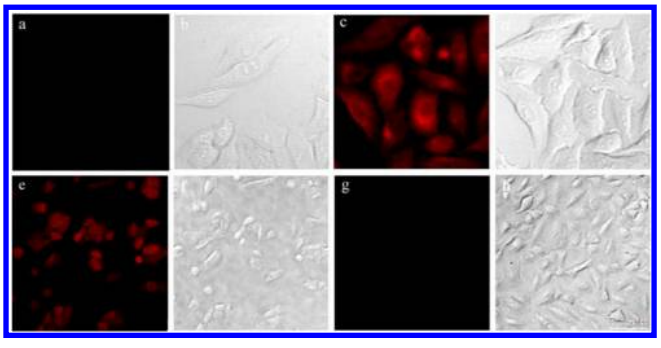

Figure 4. Confocal fluorescence images in living cells: (a) image of HepG2 cells incubated with 10 μM PAC; (b) bright-field image of (a); (c) image of HepG2 cells incubated with 10 μM PAC and 50 μM NaHS; (d) bright-field image of (c); (e) image of A549 cells incubated with 500 μM SNP and 10 μM PAC; (f) bright-field image of (e); (g) image of A549 cells incubated with 250 mg·L^{-1} PPG and 10 μM PAC; (h) bright-field image of (g).

After the capability estimation of the probe PAC for exogenous H_2S detection in living cells, we further employed the probe to detect endogenic H_2S in A549 cells, whose redox signaling has been found to be relative to that of H_2S.[52] In A549 cells, the relatively high contents of the enzymes cystathionine β-synthase (CBS) and cystathionine γ-lyase (CSE) are important for H_2S synthesis.[52] It has also been demonstrated that NO could upregulate the activity of CSE and CBS.[25] In addition, our experiment on selectivity emphasized the probe's high selectivity toward H_2S over NO.

Therefore, we selected a commercial NO donor (SNP) to induce the generation of H_2S in A549 cells. A549 cells incubated with 500 μM SNP for 60 min were referred to as SNP–A549. As can be seen from Figure 4e,f, after coincubation of SNP-A549 cells with 10 μM PAC for another 30 min, significant fluorescence enhancement was observed. Inversely, while DL-propargylglycine (PPG; 250 mg·L^{-1}), an inhibitor of CBS and CSE,[53] was added before the cells were stimulated by SNP, no significant fluorescence of the cells was observed after coincubation of SNP–A549 cells with 10 μM PAC in similar conditions with no inhibitor (Figure 4g,h). The results indicated that this nano-MOF probe was able to detect H_2S in living cells.

CONCLUSIONS

We have presented a Cu(II)-metalated noninterpenetrated 3D porous metal–organic framework and successfully employed this nano-MOF as a novel heterogeneous fluorescence probe for H_2S detection. As far as we know, nano-MOFs have never been used as selective fluorescence probes for H_2S detection. Successfully combining the advantages of MOFs and nanomaterials, this biocompatible nano-MOF probe exhibits rapid response, excellent selectivity, and hypotoxicity in in situ detection of H_2S and has been proved to be the most sensitive H_2S probe under physiological pH. Moreover, confocal imaging was achieved successfully in living cells with this probe. This work, on one hand, illustrates the great opportunity for the development of the interface between MOFs and the probe-based luminescence imaging techniques and, on the other hand, demonstrates the great potential of finding novel and intriguing probe patterns for studying underlying molecular events involved in signaling transduction.

ASSOCIATED CONTENT

Supporting Information

Experimental details, PXRD patterns, EDS spectra, TEM images, and fluorescence spectra. This material is available free of charge via the Internet at http://pubs.acs.org.

AUTHOR INFORMATION

Corresponding Author

*E-mail: tangb@sdnu.edu.cn. Fax: (86)53186180017.

Notes

The authors declare no competing financial interest.

ACKNOWLEDGMENTS

This work was supported by the 973 Program (Grant No. 2013CB933800), the National Natural Science Foundation of China (Grants No. 21227005, 21390411, 91313302, 21035003, and 21205072), and the Specialized Research Fund for the Doctoral Program of Higher Education jointly funded project (Grant No. 20123704120005).

REFERENCES

(1) Wang, R. *FASEB J.* **2002**, *16*, 1792−1798.
(2) Han, Y.; Qin, J.; Chang, X.; Yang, Z.; Du, J. *Cell. Mol. Neurobiol.* **2006**, *26*, 101−107.
(3) Culotta, E.; Koshland, D. E. *Science* **1992**, *258*, 1862−1865.
(4) Morita, T.; Perrella, M. A.; Lee, M. E.; Kourembanas, S. *Proc. Natl. Acad. Sci. U.S.A.* **1995**, *92*, 1475−1479.
(5) Tanizawa, K. *J. Biochem.* **2011**, *149*, 357−359.
(6) Calvert, J. W.; Jha, S.; Gundewar, S.; Elrod, W. J.; Ramachandran, A.; Pattillo, C. B.; Kevil, C. G.; Lefer, D. J. *Circ. Res.* **2009**, *105*, 365−374.
(7) Li, L.; Bhatia, M.; Zhu, Y. Z.; Zhu, Y. C.; Ramnath, R. D.; Wang, Z. J.; Anuar, F. B.; Whiteman, M.; Salto-Tellez, M.; Moore, P. K. *FASEB J.* **2005**, *19*, 1196−1198.
(8) Yang, G. D.; Wu, L. Y.; Wang, R. *FASEB J.* **2006**, *20*, 553−555.
(9) Eto, K.; Asada, T.; Arima, K.; Makifuchi, T.; Kimura, H. *Biochem. Biophys. Res. Commun.* **2002**, *293*, 1485−1488.
(10) Kamoun, P.; Belardinelli, M.-C.; Chabli, A.; Lallouchi, K.; Chadefaux-Vekemans, B. *Am. J. Med. Genet.* **2003**, *116A*, 310−311.
(11) Radford-Knoery, J.; Cutter, G. A. *Anal. Chem.* **1993**, *65*, 976−982.
(12) Furne, J.; Saeed, A.; Levitt, M. D. *Am. J. Physiol.* **2008**, *295*, R1479−R1485.
(13) Choi, M. G.; Cha, S.; Lee, H.; Jeon, H. L.; Chang, S. K. *Chem. Commun.* **2009**, 7390−7392.
(14) Jimnez, D.; Martinez-Manez, R.; Sancenon, F.; Ros-Lis, J. V.; Benito, A.; Soto, J. *J. Am. Chem. Soc.* **2003**, *125*, 9000−9001.
(15) Searcy, D. G.; Peterson, M. A. *Anal. Biochem.* **2004**, *324*, 269−275.
(16) Lawrence, N. S.; Davis, J.; Jiang, L.; Jones, T. G. J.; Davies, S. N.; Compton, R. G. *Electroanalysis* **2000**, *18*, 1453−1460.
(17) Zhang, W.; Li, P.; Yang, F.; Hu, X. F.; Sun, C. Z.; Zhang, W.; Chen, D. Z.; Tang, B. *J. Am. Chem. Soc.* **2013**, *135*, 14956−14959.
(18) Xu, K. H.; Qiang, M. M.; Gao, W.; Su, R. X.; Li, N.; Gao, Y.; Xie, Y. X.; Kong, F. P.; Tang, B. *Chem. Sci.* **2013**, *4*, 1079−1086.
(19) Niu, L. Y.; Guan, Y. S.; Chen, Y. Z.; Wu, L. Z.; Tung, C. H.; Yang, Q. Z. *J. Am. Chem. Soc.* **2012**, *134*, 18928−18931.
(20) Lippert, A. R.; New, R. J.; Chang, C. J. *J. Am. Chem. Soc.* **2011**, *133*, 10078−10080.
(21) Peng, H.; Cheng, Y.; Dai, C.; King, A. L.; Predmore, B. L.; Lefer, D. J.; Wang, B. *Angew. Chem.* **2011**, *123*, 9846−9849; *Angew. Chem., Int. Ed.* **2011**, *50*, 9672−9675.
(22) Das, S. K.; Lim, C. S.; Yang, S. Y.; Han, J. H.; Cho, B. R. *Chem. Commun.* **2012**, *48*, 8395−8397.
(23) Chen, S.; Chen, Z.; Ren, W.; Ai, H. *J. Am. Chem. Soc.* **2012**, *134*, 9589−9592.
(24) Wan, Q.; Song, Y.; Li, Z.; Gao, X.; Ma, H. *Chem. Commun.* **2013**, *49*, 502−504.
(25) Wu, Z.; Li, Z.; Yang, L.; Han, J.; Han, S. *Chem. Commun.* **2012**, *48*, 10120−10122.
(26) Montoya, L. A.; Pluth, M. D. *Chem. Commun.* **2012**, *48*, 4767−4769.
(27) Wang, R.; Yu, F.; Chen, L.; Chen, H.; Wang, L.; Zhang, W. *Chem. Commun.* **2012**, *48*, 11757−11759.
(28) Xuan, W.; Pan, R.; Cao, Y.; Liu, K.; Wang, W. *Chem. Commun.* **2012**, *48*, 10669−10671.
(29) Wu, M. Y.; Li, K.; Hou, J. T.; Huang, Z.; Yu, X. Q. *Org. Biomol. Chem.* **2012**, *10*, 8342−8347.
(30) Yu, F. B.; Li, P.; Song, P.; Wang, B. S.; Zhao, J. Z.; Han, K. L. *Chem. Commun.* **2012**, *48*, 2852−2854.
(31) Liu, C.; Pan, J.; Li, S.; Zhao, Y.; Wu, L. Y.; Berkman, C. E.; Whorton, A. R.; Xian, M. *Angew. Chem.* **2011**, *123*, 10511−10513; *Angew. Chem., Int. Ed.* **2011**, *50*, 10327−10329.
(32) Liu, C.; Peng, B.; Li, S.; Park, C.-M.; Whorton, A. R.; Xian, M. *Org. Lett.* **2012**, *14*, 2184−2187.
(33) Qian, Y.; Karpus, J.; Kabil, O.; Zhang, S.-Y.; Zhu, H.-L.; Banerjee, R.; Zhao, J.; He, C. *Nat. Commun.* **2011**, *2*, 495−501.
(34) Qian, Y.; Zhang, L.; Ding, S.; Deng, X.; He, C.; Zhu, H.-L.; Zhao, J. *Chem. Sci.* **2012**, *3*, 2920−2923.
(35) Xu, Z.; Xu, L.; Zhou, J.; Xu, Y.; Zhu, W.; Qian, X. *Chem. Commun.* **2012**, *48*, 10871−10873.
(36) Wang, X.; Sun, J.; Zhang, W. H.; Ma, X. X.; Lv, J. Z.; Tang, B. *Chem. Sci.* **2013**, *4*, 2551−2556.
(37) Sasakura, K.; Hanaoka, K.; Shibuya, N.; Mikami, Y.; Kimura, Y.; Komatsu, T.; Ueno, T.; Terai, T.; Kimura, H.; Nagano, T. *J. Am. Chem. Soc.* **2011**, *133*, 18003−18005.
(38) Hou, F.; Huang, L.; Xi, P.; Cheng, J.; Zhao, X.; Xie, G.; Shi, Y.; Cheng, F.; Yao, X.; Bai, D.; Zeng, Z. *Inorg. Chem.* **2012**, *51*, 2454−2460.
(39) Hou, F. P.; Cheng, J.; Xi, P. X.; Chen, F. J.; Huang, L.; Xie, G. Q.; Shi, Y. J.; Liu, H. Y.; Bai, D. C.; Zeng, Z. Z. *Dalton Trans.* **2012**, *41*, 5799−5804.
(40) Wang, J. L.; Long, L. P.; Xie, D.; Zhan, Y. W. *J. Lumin.* **2013**, *139*, 40−46.
(41) Cao, X. W.; Lin, W. Y.; Zheng, K.; He, L. W. *Chem. Commun.* **2012**, *48*, 10529−10531.
(42) Wang, J. L.; Lin, W. Y.; Li, W. L. *Biomaterials* **2013**, *34*, 7429−7436.
(43) Barnett, S. A.; Champness, N. R. *Coord. Chem. Rev.* **2003**, *246*, 145−168.
(44) Roesky, H. W.; Andruh, M. *Coord. Chem. Rev.* **2003**, *236*, 91−119.
(45) Gu, Z. Y.; Yang, C. X.; Chang, N.; Yan, X. P. *Acc. Chem. Res.* **2012**, *45*, 734−745.
(46) Yang, C. X.; Ren, H. B.; Yan, X. P. *Anal. Chem.* **2013**, *85*, 7441−7446.
(47) Bradshaw, J. E.; Gillogly, K. A.; Wilson, L. J.; Kumar, K.; Wan, X. M.; Tweedle, M. F.; Hernandez, G.; Bryant, R. G. *Inorg. Chim. Acta* **1998**, *275*−*276*, 106−l16.
(48) Li, H. W.; Feng, X.; Guo, Y. X.; Chen, D. D.; Li, R.; Ren, X. Q.; Jiang, X.; Dong, Y. P.; Wang, B. *Sci. Rep.* **2014**, *4*, 4366−4370.
(49) Aquilanti, G.; Giorgetti, M.; Minicucci, M.; Papini, G.; Pellei, M.; Tegoni, M.; Trasattic, A.; Santini, C. *Dalton Trans.* **2011**, *40*, 2764−2777.
(50) Masoomi, M. Y.; Morsali, A. *RSC Adv.* **2013**, *3*, 19191−19218 and references therein.
(51) Fateeva, A.; Chater, P. A.; Ireland, C. P.; Tahir, A. A.; Khimyak, Y. Z.; Wiper, P. V.; Darwent, J. R.; Rosseinsky, M. J. *Angew. Chem.* **2012**, *124*, 7558−7562; *Angew. Chem., Int. Ed.* **2012**, *51*, 7440−7444.
(52) Nishida, M.; Sawa, T.; Kitajima, N.; Ono, K.; Inoue, H.; Ihara, H.; Motohashi, H.; Yamamoto, M.; Suematsu, M.; Kurose, H.; Vliet, A.; Freeman, B. A.; Shibata, T.; Uchida, K.; Kumagai, Y.; Akaike, T. *Nat. Chem. Biol.* **2012**, *8*, 714−724.
(53) Zhao, W. M.; Zhang, J.; Lu, Y. J.; Wang, R. *EMBO J.* **2001**, *20*, 6008−6016.